

Supporting Information

Infrared photodissociation spectroscopic investigation on VO^+ and NbO^+ hydrolysis Catalyzed by Water Molecules

Ke Xin^a, Yinjuan Chen^a, Luning Zhang^a, Bing Xu^a, Xuefeng Wang^{a,*}, Guanjun Wang^{b,*}

^a School of Chemical Science and Engineering, Shanghai Key Lab of Chemical Assessment and Sustainability Tongji University, 1239 Siping Road, Shanghai, 200092, China

^b Department of Chemistry, Shanghai Key Laboratory of Molecular Catalysts and Innovative Materials, Fudan University, Shanghai, 200433, China

The Supporting Information includes 14 pages with 27 figures.

Content

$\text{VO}(\text{H}_2\text{O})_n\text{Ar}^+$

Fig. S1. Geometries of the low-energy isomers of $\text{VO}(\text{H}_2\text{O})^+$.	S1
Fig. S2. Geometries of the low-energy isomers of $\text{VO}(\text{H}_2\text{O})_2^+$.	S1
Fig. S3. Geometries of the low-energy isomers of $\text{VO}(\text{H}_2\text{O})\text{Ar}^+$.	S1
Fig. S4. Geometries of the low-energy isomers of $\text{VO}(\text{H}_2\text{O})_2\text{Ar}^+$.	S1
Fig. S5. Geometries of the low-energy isomers of $\text{VO}(\text{H}_2\text{O})\text{Ar}_2^+$.	S2
Fig. S6. The experimental (Exp.) and simulated vibrational spectra of $\text{VO}(\text{H}_2\text{O})\text{Ar}^+$.	S2
Fig. S7. The experimental (Exp.) and simulated vibrational spectra of $\text{VO}(\text{H}_2\text{O})_2\text{Ar}^+$.	S3
Fig. S8. The experimental (Exp.) and simulated vibrational spectra of $\text{VO}(\text{H}_2\text{O})\text{Ar}_2^+$.	S4
Fig. S9. The experimental (Exp.) and simulated anharmonic / harmonic vibrational spectra of $\text{VO}(\text{H}_2\text{O})_2\text{Ar}^+$.	S4
Fig. S10. Potential energy surfaces for the reactions of $\text{VO}^+ + \text{H}_2\text{O} \rightarrow \text{VO}(\text{H}_2\text{O})^+$	S5
Fig. S11. Potential energy surfaces for the reactions of $\text{VO}^+ + 2\text{H}_2\text{O} \rightarrow \text{V}(\text{OH})_2(\text{H}_2\text{O})^+$	S5

$\text{NbO}(\text{H}_2\text{O})_n\text{Ar}^+$

Fig. S12. Geometries of the low-energy isomers of $\text{NbO}(\text{H}_2\text{O})^+$.	S6
Fig. S13. Geometries of the low-energy isomers of $\text{NbO}(\text{H}_2\text{O})_2^+$.	S6
Fig. S14. Geometries of the low-energy isomers of $\text{NbO}(\text{H}_2\text{O})\text{Ar}^+$.	S6
Fig. S15. Geometries of the low-energy isomers of $\text{NbO}(\text{H}_2\text{O})_2\text{Ar}^+$.	S6
Fig. S16. Geometries of the low-energy isomers of $\text{NbO}(\text{H}_2\text{O})\text{Ar}_2^+$.	S7
Fig. S17. Geometries of the low-energy isomers of $\text{NbO}(\text{H}_2\text{O})_2\text{Ar}_2^+$.	S7
Fig. S18. The experimental (Exp.) and simulated vibrational spectra of $\text{NbO}(\text{H}_2\text{O})\text{Ar}^+$.	S8
Fig. S19. The experimental (Exp.) and simulated vibrational spectra of $\text{NbO}(\text{H}_2\text{O})_2\text{Ar}^+$.	S9
Fig. S20. The experimental (Exp.) and simulated vibrational spectra of $\text{NbO}(\text{H}_2\text{O})\text{Ar}_2^+$.	S10

Fig. S21. The experimental (Exp.) and simulated vibrational spectra of $\text{NbO}(\text{H}_2\text{O})_2\text{Ar}_2^+$.	S11
Fig. S22. The experimental (Exp.) and simulated anharmonic / harmonic vibrational spectra of $\text{NbO}(\text{H}_2\text{O})\text{Ar}^+$.	S11
Fig. S23. The experimental (Exp.) and simulated anharmonic/harmonic vibrational spectra of $\text{NbO}(\text{H}_2\text{O})\text{Ar}_2^+$.	S12
Fig. S24. The experimental (Exp.) and simulated anharmonic/harmonic vibrational spectra of $\text{NbO}(\text{H}_2\text{O})_2\text{Ar}^+$.	S12
Fig. S25. The experimental (Exp.) and simulated anharmonic/harmonic vibrational spectra of $\text{NbO}(\text{H}_2\text{O})_2\text{Ar}_2^+$.	S13
Fig. S26. Potential energy surfaces for the reactions of $\text{NbO}^+ + \text{H}_2\text{O} \rightarrow \text{NbO}(\text{H}_2\text{O})^+$	S13
Fig. S27. Potential energy surfaces for the reactions of $\text{NbO}^+ + 2\text{H}_2\text{O} \rightarrow \text{HNb}(\text{OH})_3^+$	S14

VO(H₂O)_nAr⁺

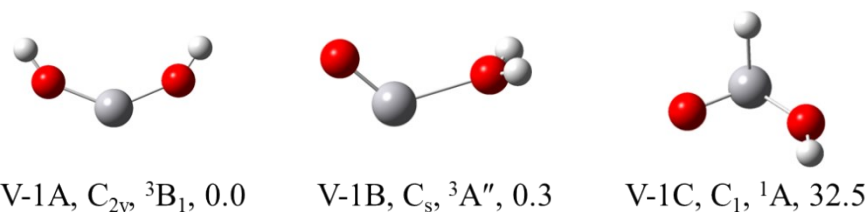


Fig. S1. Optimized structures of the minimum-energy isomers of VO(H₂O)⁺. The relative energies (with ZPE correction) are given in kcal/mol.

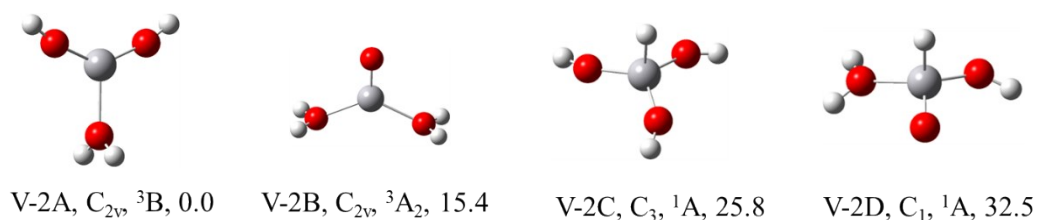


Fig. S2. Optimized structures of the minimum-energy isomers of VO(H₂O)₂⁺. The relative energies (with ZPE correction) are given in kcal/mol.

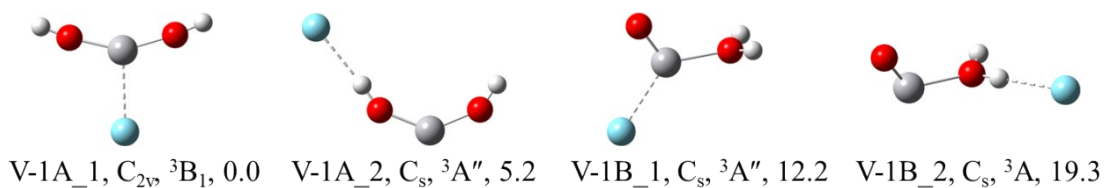


Fig. S3. Optimized structures of the minimum-energy isomers of VO(H₂O)Ar⁺. The relative energies (with ZPE correction) are given in kcal/mol.

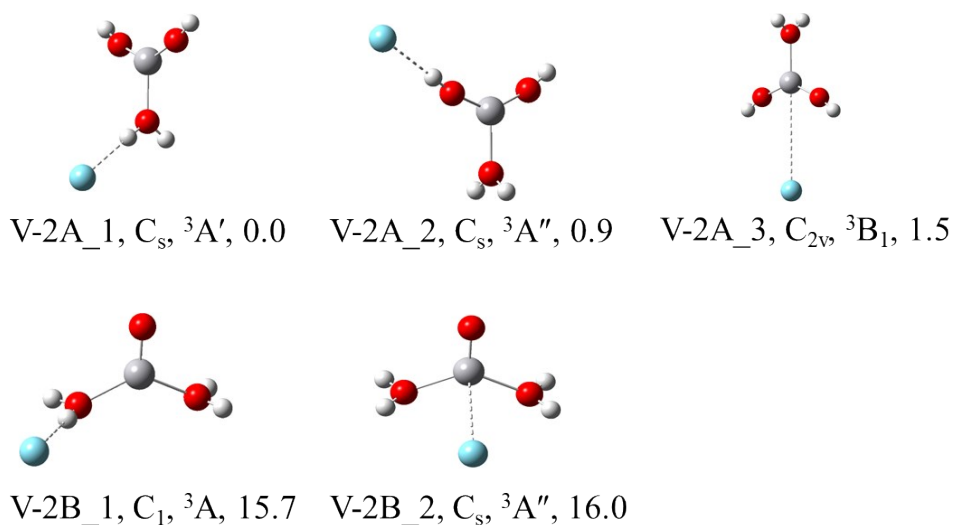


Fig. S4. Optimized structures of the minimum-energy isomers of VO(H₂O)₂Ar⁺. The relative energies (with ZPE correction) are given in kcal/mol.

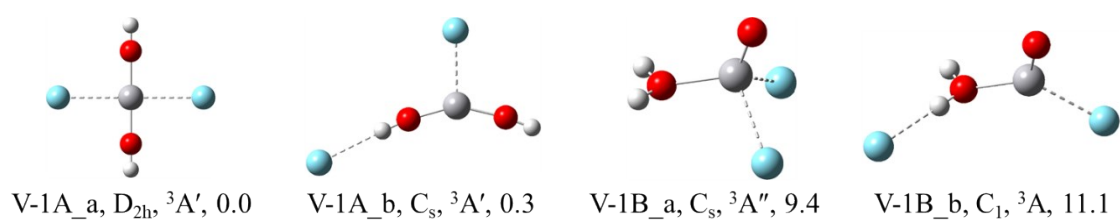


Fig. S5. Optimized structures of the minimum-energy isomers of $VO(H_2O)Ar_2^+$. The relative energies (with ZPE correction) are given in kcal/mol.

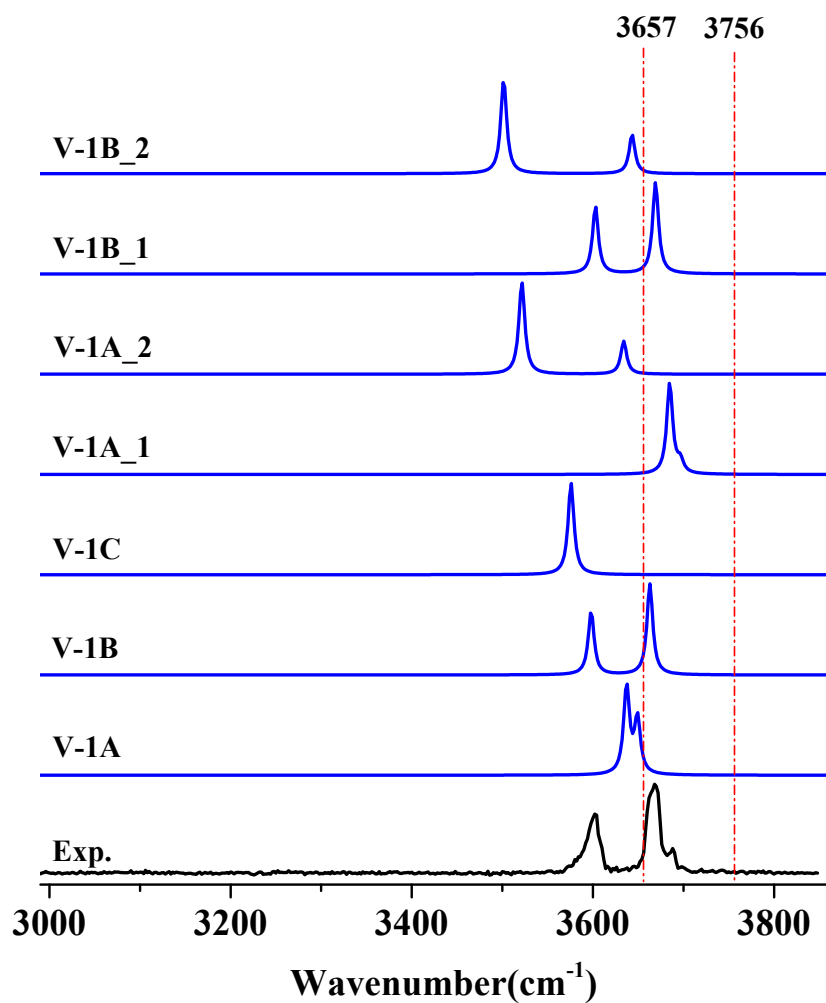


Fig. S6. Experimental infrared spectrum (black) and simulated vibrational spectra (blue) of $VO(H_2O)Ar^+$ in O-H stretching frequency region. The two dashed red lines are corresponding to the symmetric ($3657cm^{-1}$) and asymmetric ($3756 cm^{-1}$) stretches of the isolated water molecule.

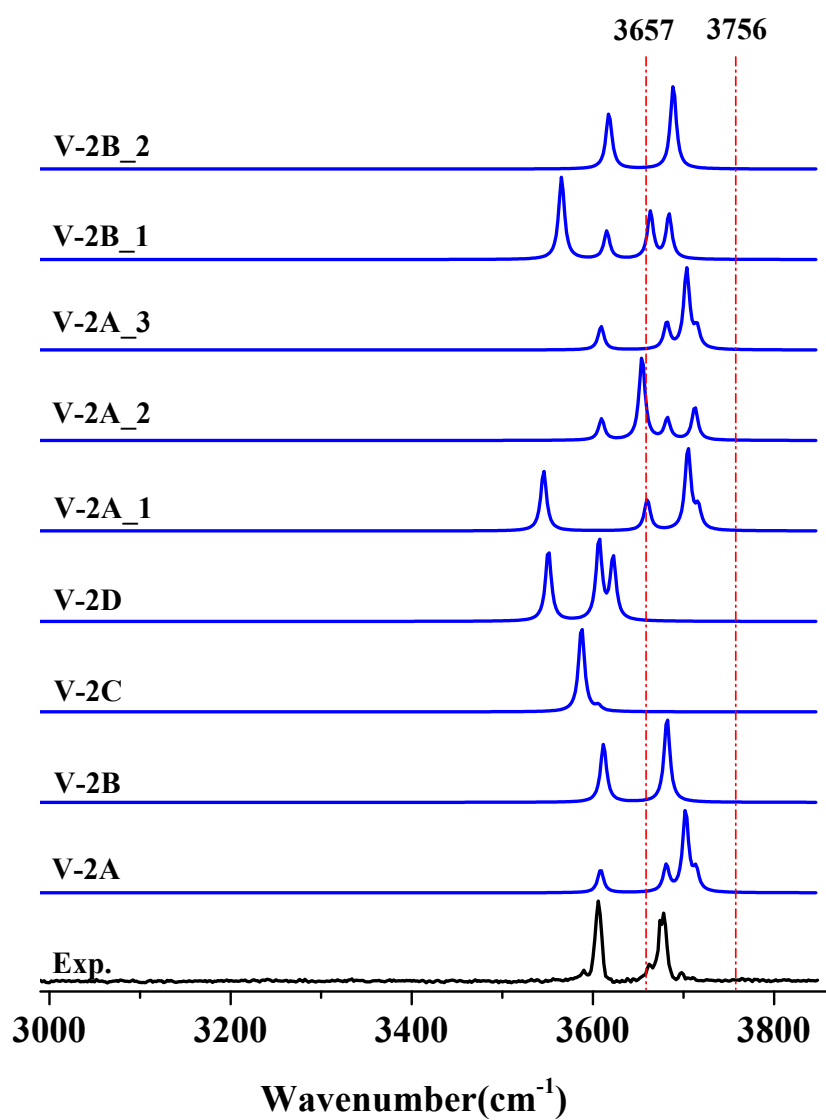


Fig. S7. Experimental infrared spectrum (black) and simulated vibrational spectra (blue) of $\text{VO}(\text{H}_2\text{O})_2\text{Ar}^+$ in O-H stretching frequency region. The two dashed red lines are corresponding to the symmetric (3657cm^{-1}) and asymmetric (3756cm^{-1}) stretches of the isolated water molecule.

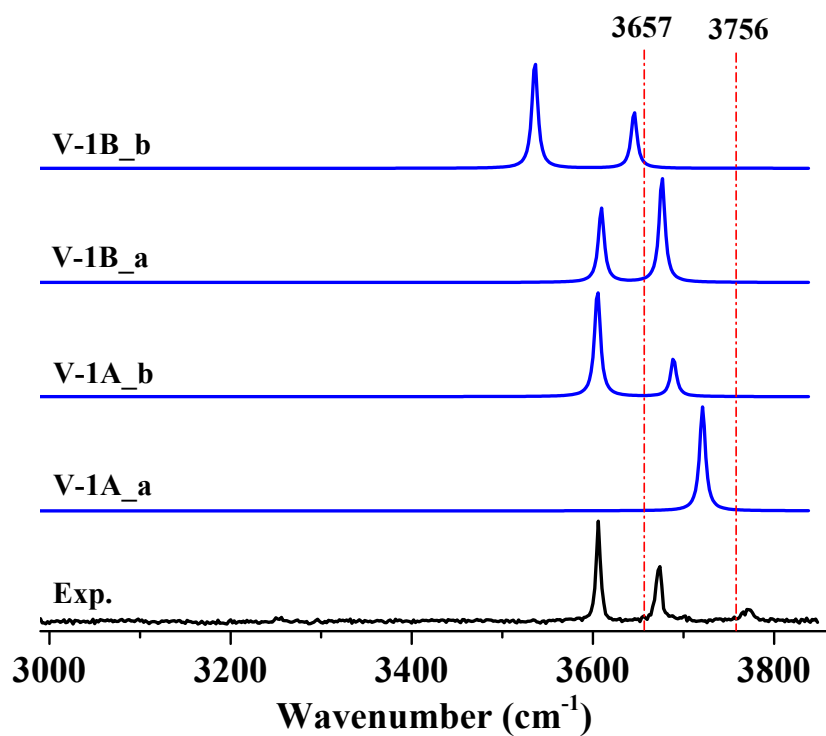


Fig. S8. Experimental infrared spectrum (black) and simulated vibrational spectra (blue) of $\text{VO}(\text{H}_2\text{O})_2\text{Ar}_2^+$ in O-H stretching frequency region. The two dashed red lines are corresponding to the symmetric (3657cm^{-1}) and asymmetric (3756cm^{-1}) stretches of the isolated water molecule.

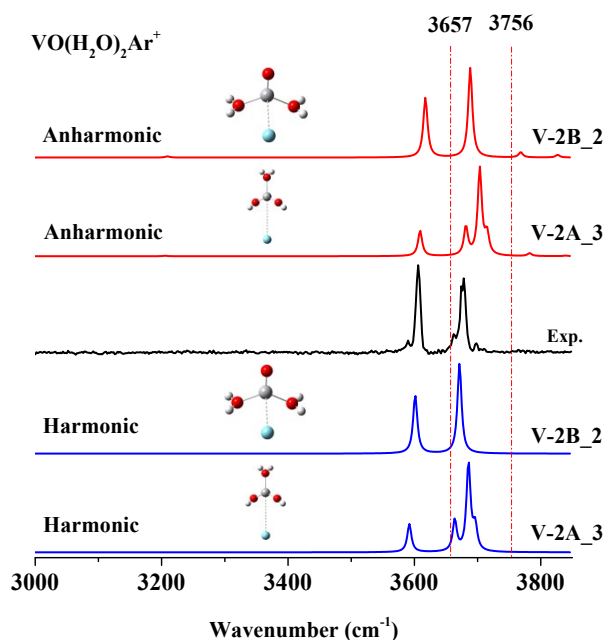


Fig. S9. Experimental infrared spectrum (black) of $\text{VO}(\text{H}_2\text{O})_2\text{Ar}_2^+$, calculated anharmonic vibrational spectrum (red) and harmonic vibrational spectrum (blue) of V-2A_3 and V-2B_2 in O-H stretching frequency region. The two dashed red lines are corresponding to the symmetric (3657cm^{-1}) and asymmetric (3756cm^{-1}) stretches of the isolated water molecule.

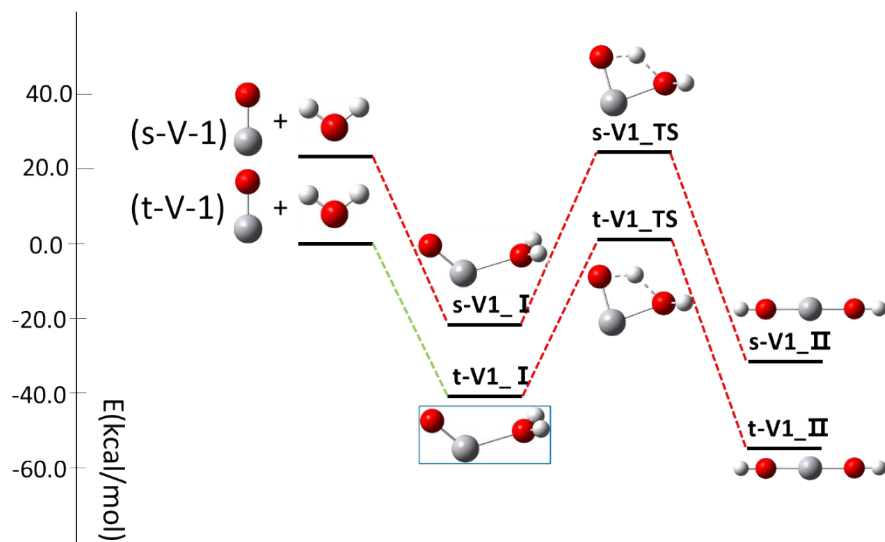


Fig. S10. Potential energy surfaces for the reactions of $\text{VO}^+ + \text{H}_2\text{O} \rightarrow \text{VO}(\text{H}_2\text{O})^+$ (s-V-1: Singlet State; t-V-1: Triplet State).

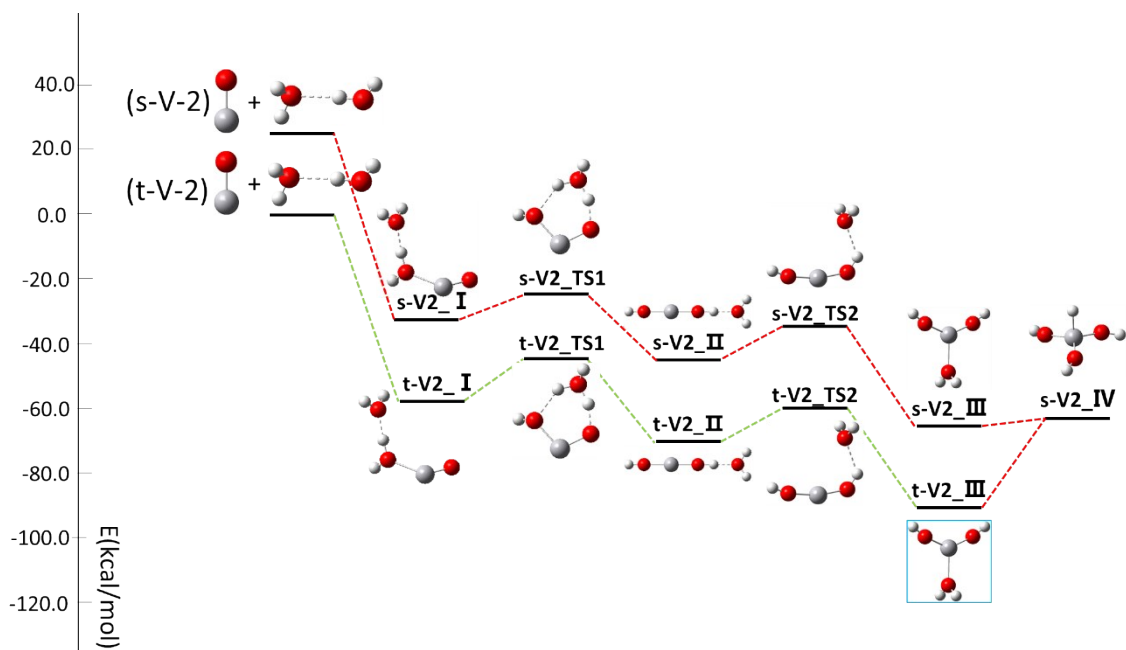


Fig. S11. Potential energy surfaces for the reactions of $\text{VO}^+ + 2\text{H}_2\text{O} \rightarrow \text{V}(\text{OH})_2(\text{H}_2\text{O})^+$ (s-V-2: Singlet State; t-V-2: Triplet State).

NbO(H₂O)_nAr⁺

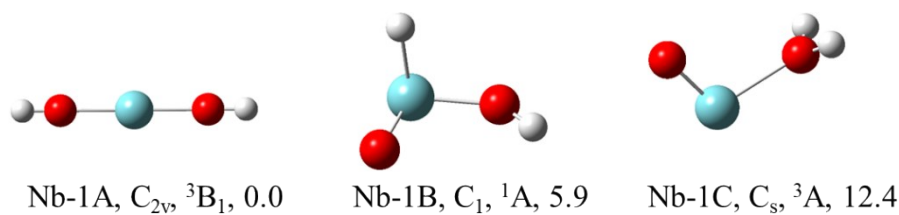


Fig. S12. Optimized structures of the minimum-energy isomers of NbO(H₂O)⁺. The relative energies (with ZPE correction) are given in kcal/mol.

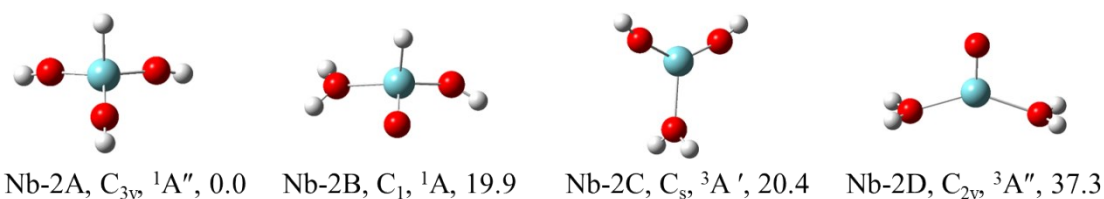


Fig. S13. Optimized structures of the minimum-energy isomers of NbO(H₂O)₂⁺. The relative energies (with ZPE correction) are given in kcal/mol.

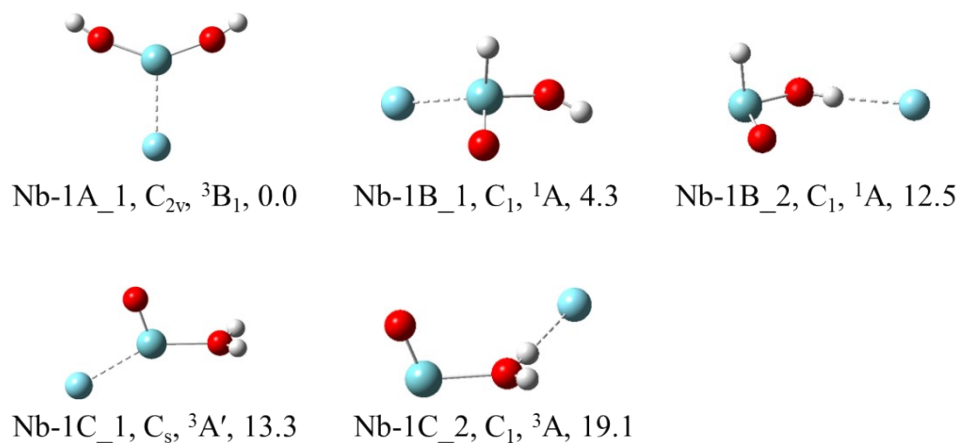


Fig. S14. Optimized structures of the minimum-energy isomers of NbO(H₂O)Ar⁺. The relative energies (with ZPE correction) are given in kcal/mol.

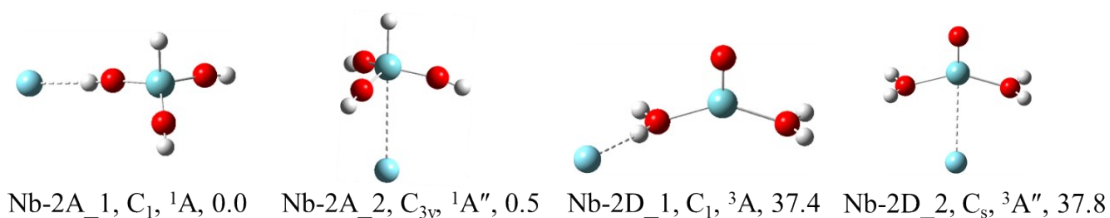


Fig. S15. Optimized structures of the minimum-energy isomers of NbO(H₂O)₂Ar⁺. The relative energies (with ZPE correction) are given in kcal/mol.

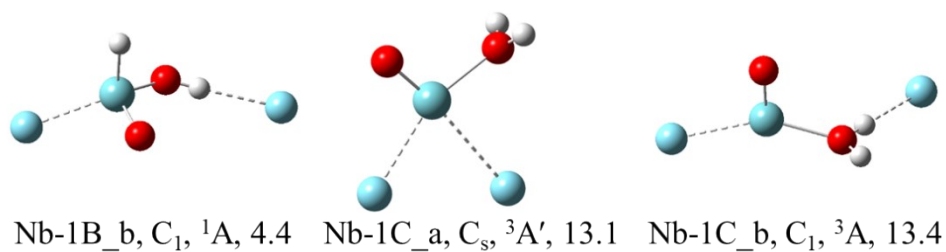
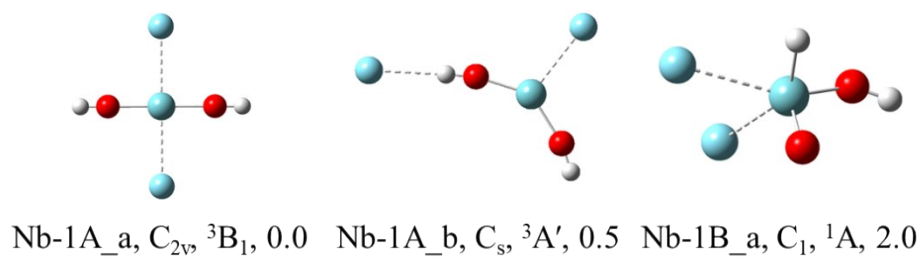


Fig. S16. Optimized structures of the minimum-energy isomers of $NbO(H_2O)Ar_2^+$. The relative energies (with ZPE correction) are given in kcal/mol.

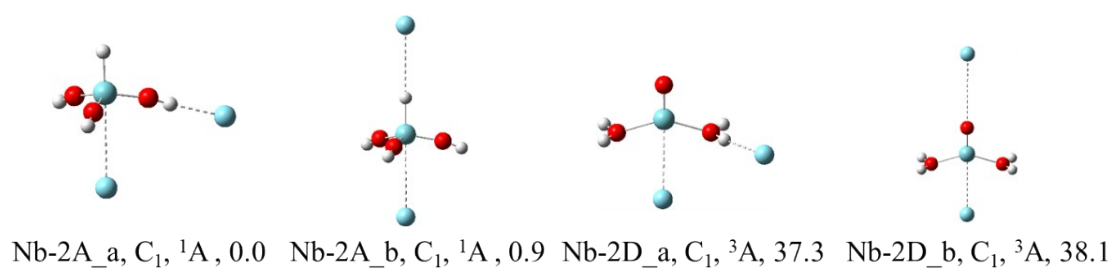


Fig. S17. Optimized structures of the minimum-energy isomers of $NbO(H_2O)_2Ar_2^+$. The relative energies (with ZPE correction) are given in kcal/mol.

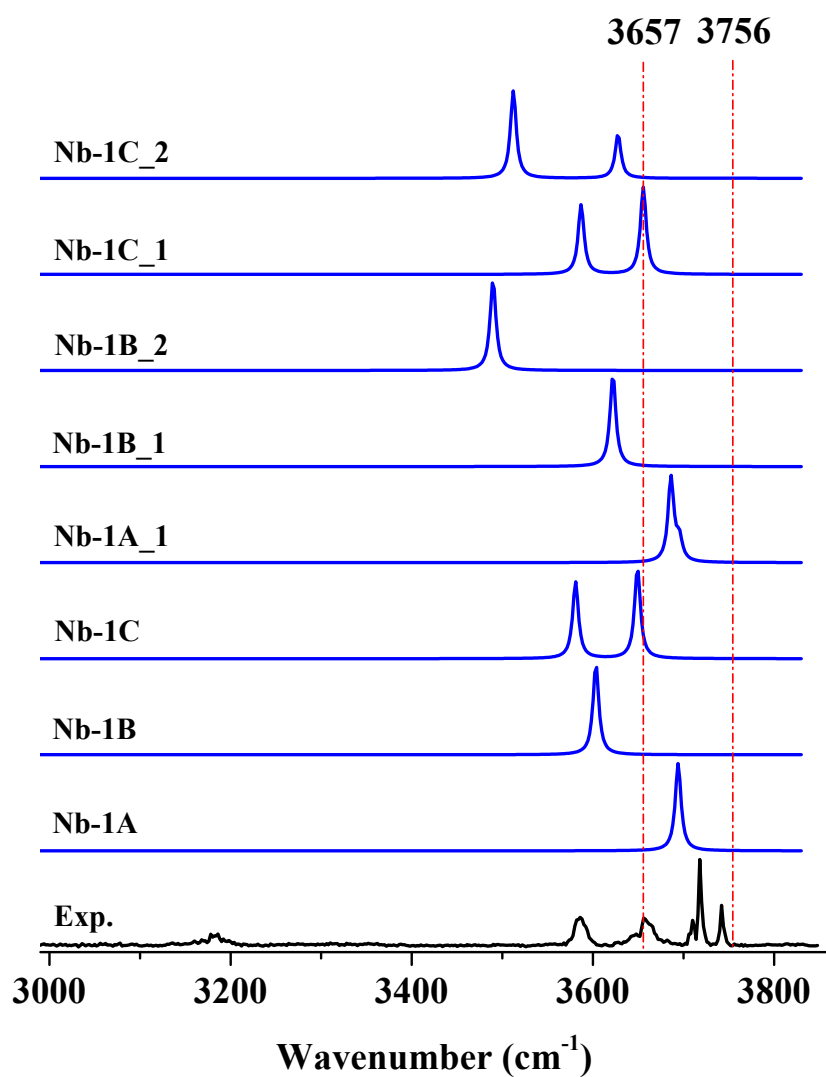


Fig. S18. Experimental infrared spectrum (black) and simulated vibrational spectra (blue) of $\text{NbO}(\text{H}_2\text{O})\text{Ar}^+$ in O-H stretching frequency region. The two dashed red lines are corresponding to the symmetric (3657cm^{-1}) and the asymmetric (3756 cm^{-1}) stretches of the isolated water molecule.

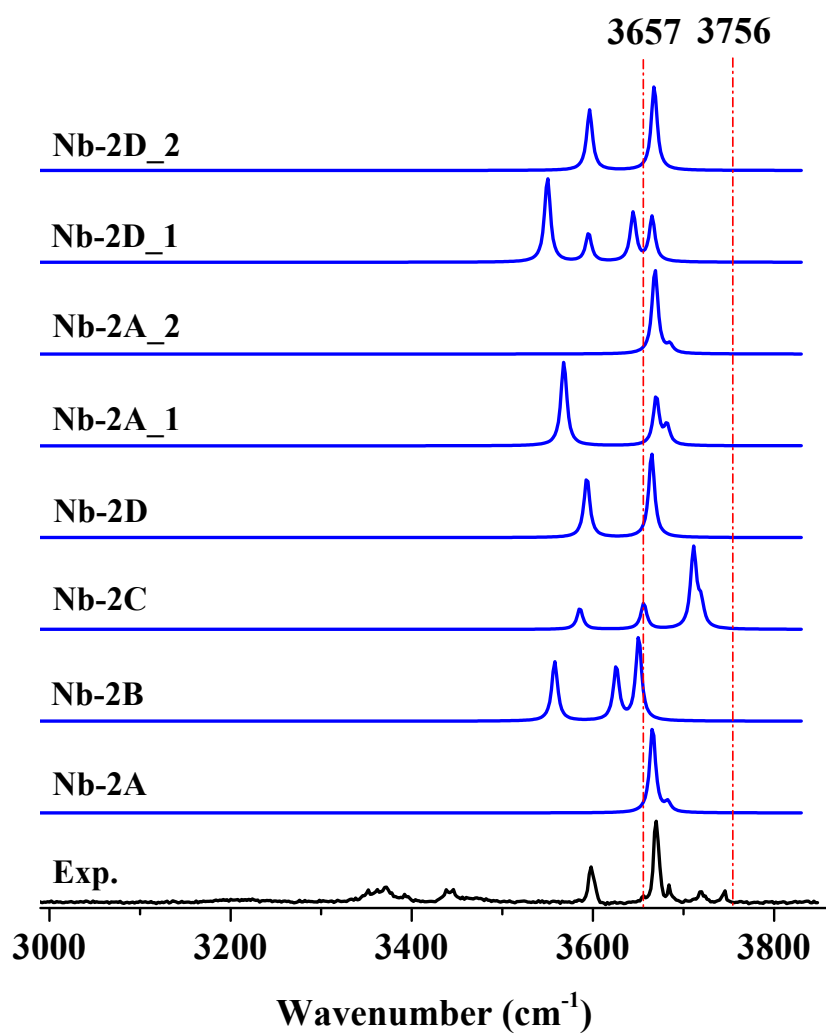


Fig. S19. Experimental infrared spectrum (black) and simulated vibrational spectra (blue) of $\text{NbO}(\text{H}_2\text{O})_2\text{Ar}^+$ in O-H stretching frequency region. The two dashed red lines are corresponding to the symmetric (3657cm^{-1}) and asymmetric (3756 cm^{-1}) stretches of the isolated water molecule.

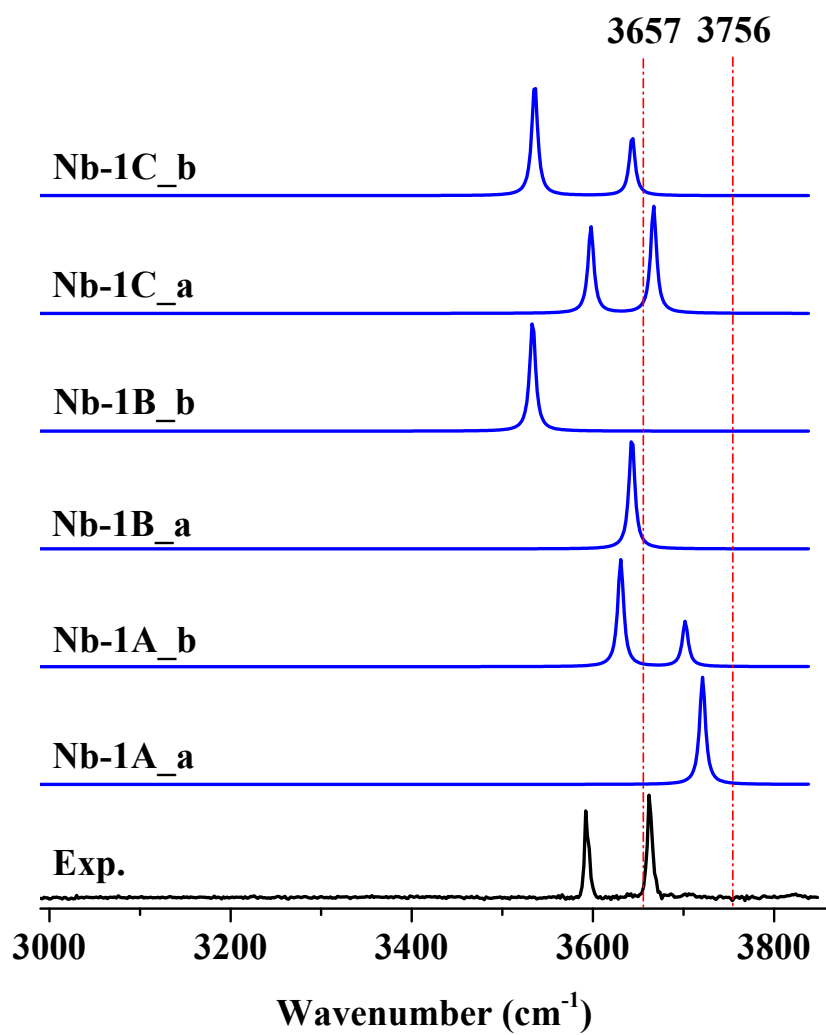


Fig. S20. Experimental infrared spectrum (black) and simulated vibrational spectra (blue) of $\text{NbO}(\text{H}_2\text{O})\text{Ar}_2^+$ in O-H stretching frequency region. The two dashed red lines are corresponding to the symmetric (3657cm^{-1}) and asymmetric (3756 cm^{-1}) stretches of the isolated water molecule.

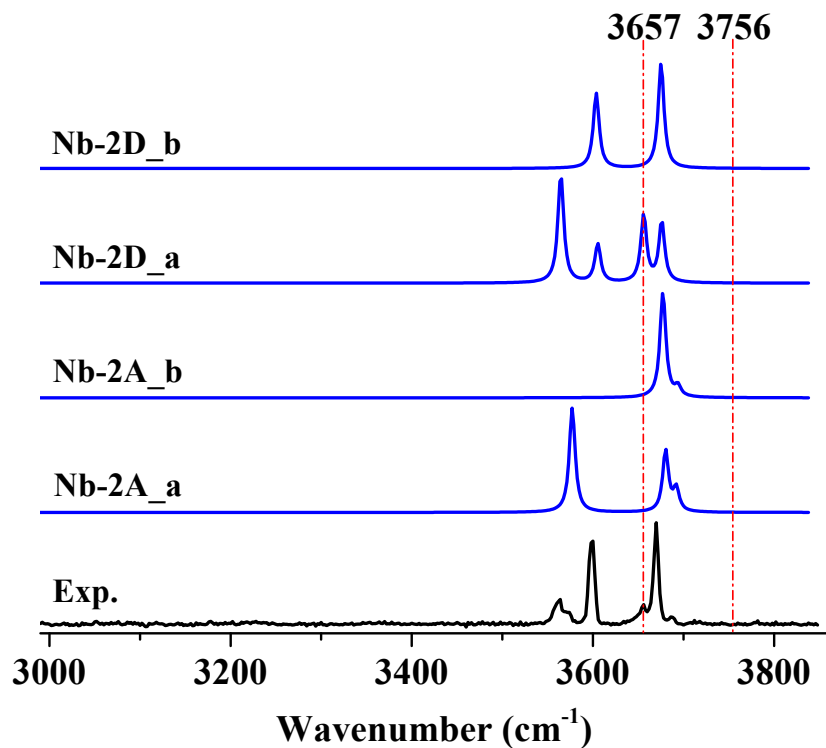


Fig. S21. Experimental infrared spectrum (black) and simulated vibrational spectra (blue) of $\text{NbO}(\text{H}_2\text{O})_2\text{Ar}_2^+$ in O-H stretching frequency region. The two dashed red lines are corresponding to the symmetric (3657cm^{-1}) and asymmetric (3756 cm^{-1}) stretches of the isolated water molecule.

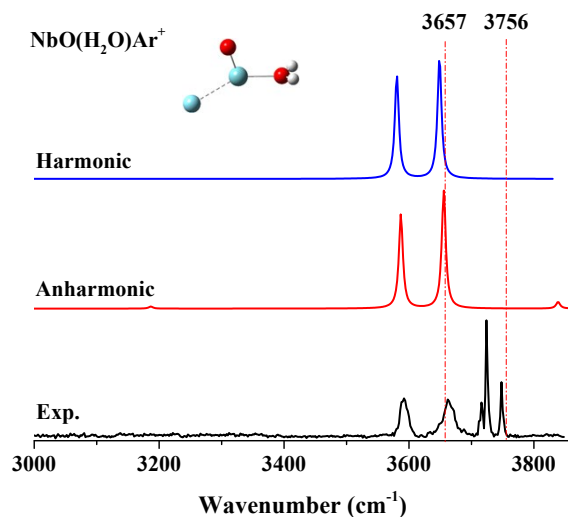


Fig. S22. Experimental infrared spectrum (black) of $\text{NbO}(\text{H}_2\text{O})\text{Ar}^+$, calculated anharmonic vibrational spectrum (red) and harmonic vibrational spectrum (blue) of Nb-1C_1 in O-H stretching frequency region. The two dashed red lines are corresponding to the symmetric (3657cm^{-1}) and asymmetric (3756 cm^{-1}) stretches of the isolated water molecule.

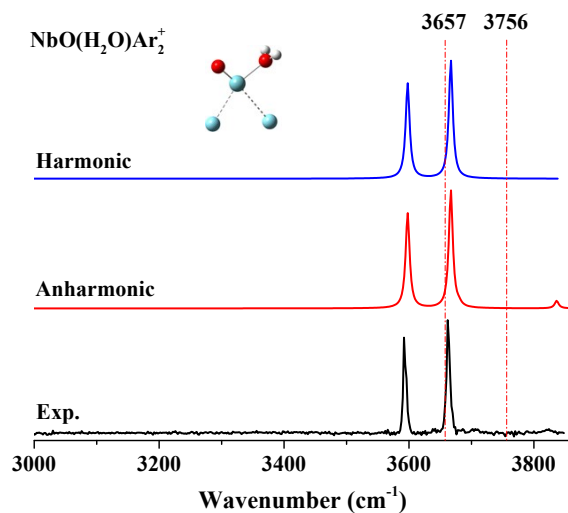


Fig. S23. Experimental infrared spectrum (black) of $\text{NbO}(\text{H}_2\text{O})\text{Ar}_2^+$, calculated anharmonic vibrational spectrum (red) and harmonic vibrational spectrum (blue) of Nb-1C_a in O-H stretching frequency region. The two dashed red lines are corresponding to the symmetric (3657 cm^{-1}) and asymmetric (3756 cm^{-1}) stretches of the isolated water molecule.

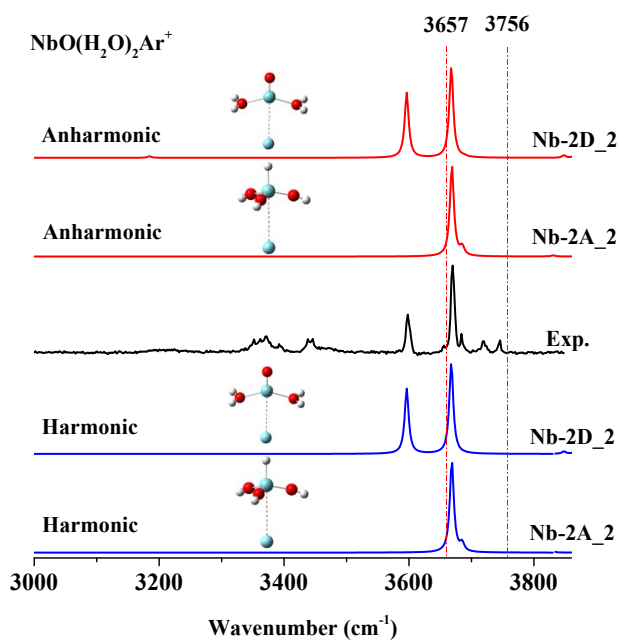


Fig. S24. Experimental infrared spectrum (black) of $\text{NbO}(\text{H}_2\text{O})_2\text{Ar}^+$, calculated anharmonic vibrational spectrum (red) and harmonic vibrational spectrum (blue) of Nb-2A_2 and Nb-2D_2 in O-H stretching frequency region. The two dashed red lines are corresponding to the symmetric (3657 cm^{-1}) and asymmetric (3756 cm^{-1}) stretches of the isolated water molecule.

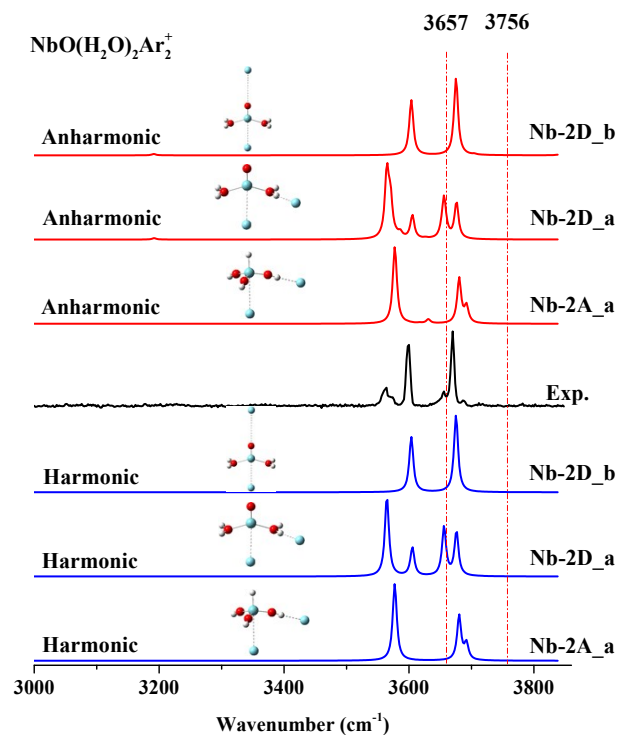


Fig. S25. Experimental infrared spectrum (black) of $\text{NbO}(\text{H}_2\text{O})_2\text{Ar}_2^+$, calculated anharmonic vibrational spectrum (red) and harmonic vibrational spectrum (blue) of Nb-2A_a, Nb-2D_a and Nb-2D_b in O-H stretching frequency region. The two dashed red lines are corresponding to the symmetric (3657 cm^{-1}) and asymmetric (3756 cm^{-1}) stretches of the isolated water molecule.

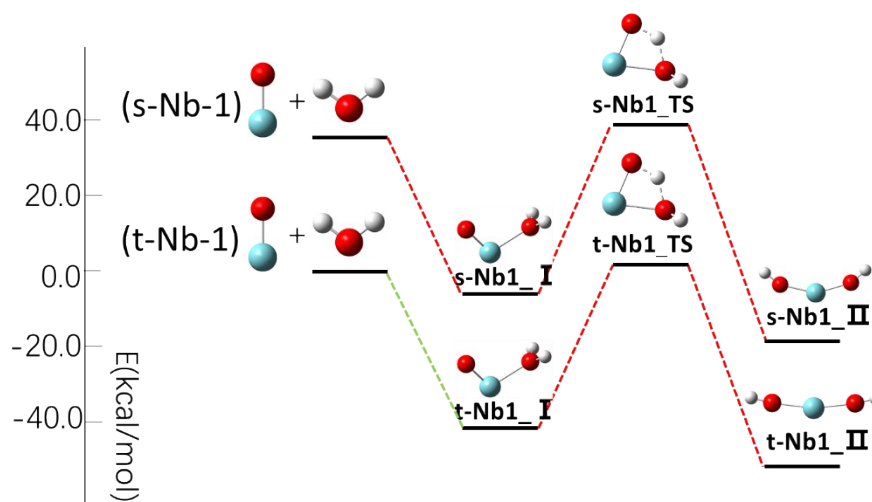


Fig. S26. Potential energy surfaces for the reactions of $\text{NbO}^+ + \text{H}_2\text{O} \rightarrow \text{NbO}(\text{H}_2\text{O})^+$ (s-Nb-1: Singlet State; t-Nb-1: Triplet State).

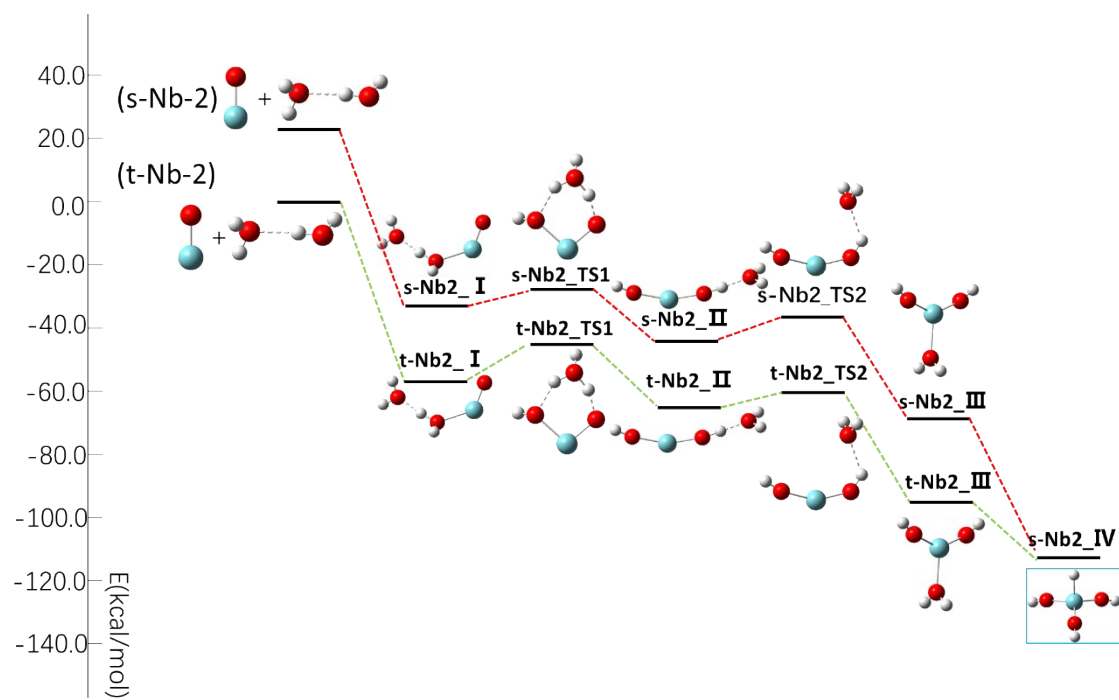


Fig. S27. Potential energy surfaces for the reactions of $\text{NbO}^+ + 2\text{H}_2\text{O} \rightarrow \text{HNb}(\text{OH})_3^+$ (s-Nb-2: Singlet State; t-Nb-2: Triplet State).